In this study, we have presented a new example, solubility, of physical properties of polymers that can be controlled reversibly by selection of the irradiating wavelength. We can expect to control reversibly many other aspects of the properties of polymers by using photoresponsive polymers.

Registry No. PS-A, 35176-66-0.

References and Notes

(1) Part 4: Irie, M.; Hayashi, K.; Menju, A. *Polym. Photochem.* **1981**, *1*, 233.
(2) Lovrien, R. *Proc. Natl. Acad. Sci. U.S.A.* **1967**, *57*, 236. Van der Veen, G.; Prins, W. *Photochem. Photobiol.* **1974**, *19*, 191, 197.
(3) Irie, M.; Menju, A.; Hayashi, K. *Macromolecules* **1979**, *12*, 1176.
(4) Irie, M.; Hirano, K.; Hashimoto, S.; Hayashi, K. *Macromolecules* **1981**, *14*, 262.
(5) Menju, A.; Hayashi, K.; Irie, M. *Macromolecules* **1981**, *14*, 755.
(6) Irie, M.; Schnabel, W. *Macromolecules* **1981**, *14*, 1246.
(7) Eisenbach, C. S. *Makromol. Chem.* **1978**, *179*, 2507.
(8) Zimmerman, G.; Chow, L.; Paik, U. *J. Am. Chem. Soc.* **1958**, *80*, 3528.
(9) Ohono, N.; Okuda, T.; Nitta, K.; Sugai, S. *J. Polym. Sci., Polym. Phys. Ed.* **1978**, *16*, 513.
(10) Bullock, D. J. W.; Cumper, C. W. N.; Vogel, I. *J. Chem. Soc.* **1965**, 5316.
(11) Schulz, G. V.; Baumann, H. *Makromol. Chem.* **1963**, *60*, 120.
(12) Stockmayer, W. H. *J. Chem. Phys.* **1945**, *13*, 199.
(13) Kihara, H.; Schnabel, W. *Z. Naturforsch., A* **1980**, *35a*, 217.

Analysis and Dilute Solution Properties of 12- and 18-Arm-Star Polystyrenes†

Jacques Roovers,*,‡ Nikos Hadjichristidis,§ and Lewis J. Fetters‖

Chemistry Division, National Research Council of Canada, Ottawa, Ontario, Canada K1A 0R9, Industrial Chemistry Department, University of Athens, Athens (144), Greece, and the Institute of Polymer Science, The University of Akron, Akron, Ohio 44325.
Received March 22, 1982

ABSTRACT: The homogeneity of samples of 12-arm- and 18-arm-star polystyrenes was investigated by ultracentrifugation sedimentation in a Θ solvent and with gel permeation chromatography combined with low-angle laser light scattering. The former method permits the detection of star polymers with different numbers of arms in a sample, and the latter allows the determination of the number of arms in the stars. Light scattering studies revealed that the star polymer coils are expanded from the random walk size in a Θ solvent for the linear polymer. The strong upward curvature at $\mu > 4$ in the reciprocal scattering curve of the stars in a good solvent suggests that the average segment density distribution in the stars is more uniform than predicted by the random walk model. Sedimentation velocity and intrinsic viscosity measurements indicate that these highly branched polymers behave hydrodynamically almost like hard spheres in dilute solution.

Introduction

Star polymers are ideally suited for the study of the relation between the segment density in polymer coils and the physical properties of the polymers, because they allow the segment density to be changed without a concomitant change in the molecular weight of the polymer.[1,2] Initially, only stars with three, four, or six equal arms could be synthesized by the rigorous method of linking monodisperse living anionic polymers with multifunctional chlorosilanes.[3] Star polymers with more than six arms were prepared by coupling living polymers through divinylbenzene nodules. This method does not allow one to predict accurately the number of arms of the stars, nor does it yield polymers with a uniform number of arms.[4] Recently, it has become possible to prepare 8-, 12-,[5] and 18-arm[6] stars by an extension of the chlorosilane method. However, as the number of arms increases, it becomes increasingly more difficult to ascertain the monodispersity in molecular weight and number of arms of the star polymers.

A careful analysis of two very high molecular weight samples of polystyrene with 12 and 18 arms, respectively, has been made in an attempt to identify the homogeneity in architecture and molecular weight of the samples. Light scattering experiments in a Θ solvent and in a good solvent have been made in order to probe the segment density distribution in the stars, at least at long segment–segment distances. Comparisons are made with the random flight model. Data on the intrinsic viscosities and sedimentation velocity coefficients are also included. The hydrodynamic properties of the stars are compared with their static dimensions in solution.

Experimental Section

The synthesis of the 12- and 18-arm polystyrenes was performed along the lines described for 12-arm polyisoprenes[5] and 18-arm polyisoprenes.[6] First a narrow molecular weight linear polystyrene was prepared by anionic polymerization techniques with *sec*-BuLi as the initiator. A small fraction was removed and terminated with degassed MeOH. It is the reference "arm" material. The living polystyryllithium was capped with a few units of butadiene prior to reaction with the multifunctional chlorosilane compound. The 12-arm star was prepared by linking of the arms with $Si[CH_2CH_2SiCl_3]_4$ and the 18-arm star was obtained with $[CH_2Si(CH_2CH_2SiCl_3)_3]_2$. About 50% excess living polymer was used in order to force the linking reaction to completion. The linking reaction was monitored by comparison of the high molecular weight "star" peak and the low molecular weight "arm" peak of GPC traces. The excess living polymer was terminated with degassed methanol. The polymers were extensively fractionated in order to remove the excess arm material. The 18-arm star, 18-PS1, was used as such. The 12-arm star, 12-PS1, was analyzed but was also subjected to an additional four-step fractionation at very high dilution in a mixture of benzene and methanol. This yielded two relatively pure fractions 12-PS1B1A and 12-PS1C, which were further studied.

* Issued as NRCC No. 20861.
‡ National Research Council of Canada.
§ University of Athens.
‖ Institute of Polymer Science, The University of Akron.

0024-9297/83/2216-0214$01.50/0

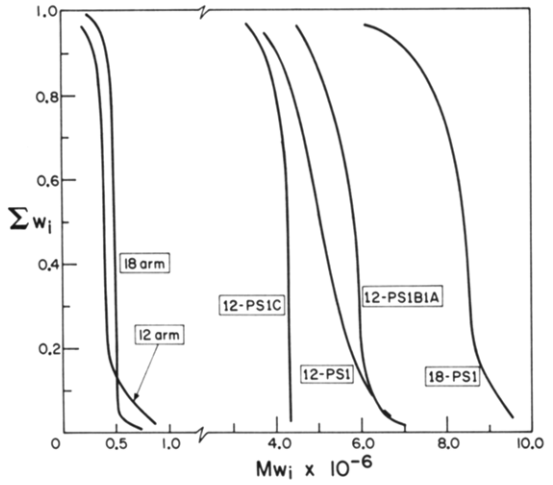

Figure 1. Cumulative molecular weight distribution of star polystyrenes as determined by GPC–LALLS.

The fractionated star samples and the arm material were analyzed with a low-angle laser light scattering instrument (LALLS Chromatix KMX-6) coupled to a size exclusion chromatograph (GPC Waters 301) with six Styragel columns of 3×10^6, 1×10^6, 3×10^5, 1×10^5, 1×10^4, and 1×10^3 Å nominal size. The eluting solvent was THF at 35 °C and the flow rate was 1.1 mL/min. The refractive index increment of polystyrene in THF at 633 nm was found to be 0.190_3 mL/g at 25 °C. The samples were also analyzed by sedimentation in a Spinco Model E analytical ultracentrifuge. The speed was 60 000 rpm and the solvent was cyclohexane at 35.0 °C. The relative amounts under the sedimenting bands were determined after extrapolation to zero concentration in order to correct for the Johnston–Ogston effect.[7]

The weight-average molecular weights of the star and the arm polymers were measured with a Fica 50 photogoniometer in cyclohexane at 34.6 °C and in toluene at 35.0 °C. For 436-nm light the refractive index increment for polystyrene is 0.181 and 0.114 in these two solvents, respectively. The Rayleigh ratio of benzene was taken as 50.8×10^{-6} at 35 °C. The radii of gyration were obtained from the zero-concentration angular dependence of the scattered light. Data obtained with 365-, 436-, 546-, and 633-nm light were combined. Details of the beam alignment and data handling have been given previously.[8] In cases of very high dissymmetry of the scattered light, a correction for back-reflection was made according to

$$R(\theta) = \frac{1}{1 - f^2}[R(\theta)_{\text{obsd}} - fR(180 - \theta)_{\text{obsd}}] \quad (1)$$

where $f = (n_1 - n_2)^2/(n_1 + n_2)^2$ and n_1 and n_2 are the refractive indices of the solution and of the solvent bath, respectively.[9]

Intrinsic viscosities were measured in semimicro Cannon-Ubbelohde viscometers with solvent flow times of about 150 s. Extrapolation to zero concentration in η_{sp}/c vs. c took into account a slight upward curvature at the highest concentrations measured, 2×10^{-3} g/mL in toluene and 4×10^{-3} g/mL in cyclohexane.

Sedimentation coefficients ($s_0°$) were determined as described previously.[10] In this case, the rotor speed was 24 000 and 20 000 rpm for 12-PS1B1A and 18-PS1, respectively. The highest concentration studied was 1.6×10^{-3} g/mL in toluene and 2.0×10^{-3} g/mL in cyclohexane. The values of $s_0°$ quoted are the experimental sedimentation coefficients extrapolated to zero concentration, after pressure correction to 1 atm and radial dilution correction.[10]

Results

The ordinary differential refractive index traces of the GPC elution peaks of the star polymers are in all cases symmetrical and indicate weight distributions that are, within experimental error, indistinguishable from those of high molecular weight narrow-distribution linear polymers. However, when the LALLS instrument is connected in line with the GPC and the instantaneous weight-average molecular weights over the star elution peaks are measured, it is found that there is substantial drift of the molecular weight for 12-PS1 (Figure 1), contrary to what is normally observed for truly monodisperse polymers. The curves for the 12- and 18-arm precursors given in Figure 1 are examples of the latter. The sedimentation pattern of 12-PS1, shown in Figure 2a, clearly indicates two major components approximately in a 1:1 weight ratio (after extrapolation to zero concentration), which correlates with the range of molecular weights observed in the GPC–LALLS analysis of that sample.

From Figure 2b, it can be seen that the high molecular weight fraction 12-PS1B1A, derived from 12-PS1, consists of the high molecular weight component contaminated by about 10% of the low molecular weight component. This is supported qualitatively by the presence of a low molecular weight tail in the GPC–LALLS trace of 12-PS1B1A (Figure 1). The low molecular weight fraction 12-PS1C (Figure 2c) is contaminated by a small amount of the high molecular weight component, which cannot be seen in the GPC–LALLS trace shown in Figure 1. Samples 12-PS1B1A and 12-PS1C were considered sufficiently pure to derive the weight-average molecular weight of the major component from their GPC–LALLS traces.

Although 18-PS1 sediments as a single band (Figure 2d) with perhaps some faster moving impurity, the GPC–LALLS pattern of this polymer shows a low molecular weight tail. Both constitute small weight fractions of the total sample. The weight-average molecular weights obtained from GPC–LALLS experiments are compared with those obtained by ordinary light scattering in cyclohexane and toluene in Table I.

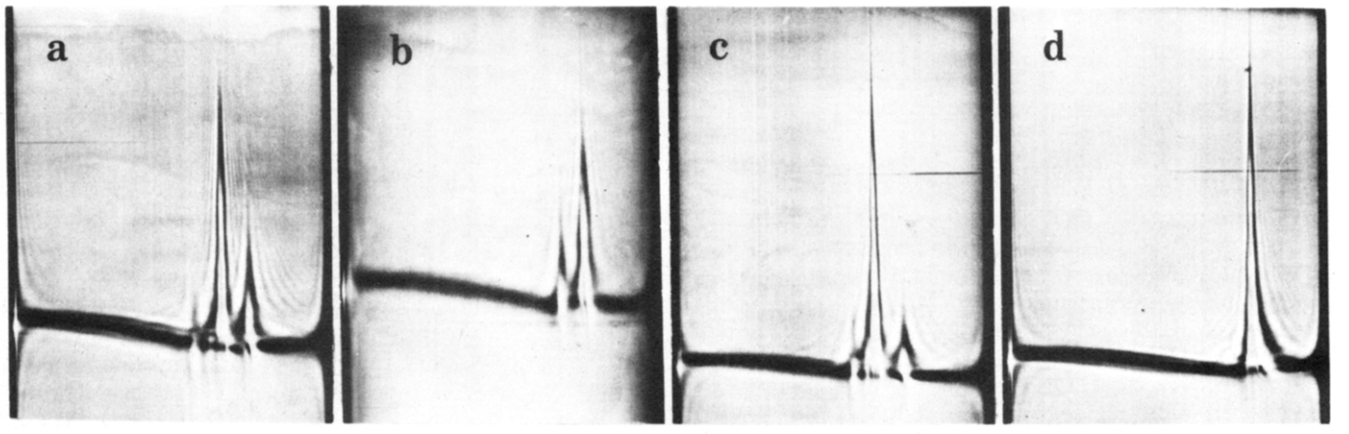

Figure 2. Ultracentrifugation sedimentation patterns of star polystyrenes in cyclohexane at 35 °C. Sedimentation is from left to right. From left to right: (a) 12-PS1 (0.2%); (b) 12-PS1B1A (0.1%); (c) 12-PS1C (0.2%); (d) 18-PS1 (0.2%).

Table I
Molecular Weight Data for Star Polystyrenes[a]

sample	$(M_w)_{GPC-LALLS}$	$(M_w)_{LS,C_6H_{12}}$	$(M_w)_{LS,C_7H_8}$	p^b
12-PS arm	0.41_5		0.43	
12-PS1B1A	5.6	5.5	5.8	12.3
18-PS arm	0.48		0.53	
18-PS1	8.2	8.9	9.3	16.8

[a] All molecular weight $\times 10^{-6}$. [b] p (number of arms) = $(M_w)_{star,C_6H_{12}}/(M_w)_{arm,C_7H_8}$.

Table II
Radii of Gyration for the Star Polystyrenes

Cyclohexane, 34.6 °C

sample	$\langle S^2\rangle_{z,\Theta}$, Å^2	g_Θ[a]	g_{rw}[b]	g_{MC}[c]	α_Θ^2	$g_\Theta p^{1/2}$
12-PS1B1A	1.2×10^5	0.27_6	0.236	0.35	1.17	0.96
18-PS1	1.6×10^5	0.22_8	0.160	0.28	1.42	0.97

Toluene, 35.0 °C

sample	$\langle S^2\rangle_z$, Å^2	g_{exptl}[d]	$A_2 \times 10^5$, (cm^3·mol)/g^2	ψ	$gp^{4/5}$
12-PS1B1A	3.3×10^5	0.24_3	8.3	1.10	1.77
18-PS1	4.8×10^5	0.20_3	5.7	1.10	2.05

[a] Equation 6. [b] Equation 4. [c] g_{MC} = ratio of radii of gyration calculated by the Monte Carlo method.[19] [d] $[\langle S^2\rangle/\langle S^2\rangle_{lin}]_M$ based on $\langle S^2\rangle_{lin} = 1.66 \times 10^{-18} M_w^{1.17}$.

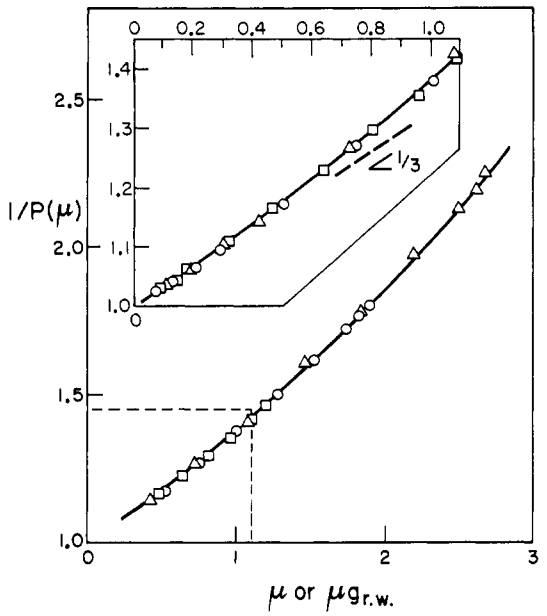

Figure 3. Inverse scattering function against μ for 12-PS1B1A in cyclohexane at 34.7 °C: (△) 366-nm light; (○) 436 nm; (□) 546 nm. The line represents the $1/P(\mu)$ function (eq 3) based on the random walk model plotted against μg_{rw}. $\langle S^2\rangle = 1.2 \times 10^5$ Å^2 and $p = 12$. The insert shows the data at low μ values.

The experimental z-average mean-square radii of gyration, $\langle S^2\rangle_z$, were derived from the zero-concentration angular dependence of the scattered light according to

$$\lim_{\substack{c\to 0\\ \theta\to 0}} \frac{c/I_\theta}{c/I_0} = 1 + \frac{16\pi^2}{3\lambda'^2}\langle S^2\rangle_z \sin^2(\theta/2) \qquad (2)$$

where I_θ and I_0 are the intensity of the scattered light at angle θ and angle zero, respectively, and λ' is the wavelength of the light in the medium. The results obtained in cyclohexane (Θ solvent) and in toluene (good solvent) are collected in Table II.

Figure 3 shows the experimental $(c/I_\theta)/(c/I_0) = 1/P(\mu)$ data as a function of $\mu = (16\pi^2/\lambda'^2)\langle S^2\rangle_z \sin^2(\theta/2)$ for 12-PS1A1B in cyclohexane measured with three different wavelengths. The solid line drawn in Figure 3 is the theoretical scattering function for a 12-arm star obeying the random walk configuration for all its subchains. For a regular star with p branches[11]

$$P(\mu) = \frac{2}{\mu} + \frac{p}{\mu}[(p-3) - 2(p-2)e^{-\mu/p} + (p-1)e^{-2\mu/p}] \qquad (3)$$

Since μ in eq 3 is defined in terms of $\langle S^2\rangle_{lin}$, the theoretical function has to be plotted against μg_{rw} in order to have the correct slope ($^1/_3$) at small μ. For regular stars[12]

$$g_{rw} = (3p-2)/p^2 \qquad (4)$$

where the subscript rw denotes the random walk model. Similarly, the experimental scattering curve for 18-PS1 in cyclohexane at the Θ temperature follows the theoretical function based on the random walk model in the range of accessible μ values. These results confirm the observations made on 12-arm polyisoprene stars.[13]

The $1/P(\mu)$ curve obtained with 18-PS1 in the good solvent toluene is shown in Figure 4. For comparison, the

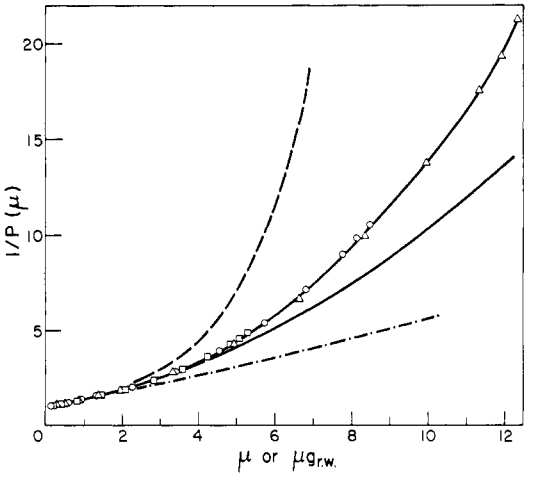

Figure 4. Inverse scattering function against μ for 18-PS1 in toluene at 35 °C. Symbols as in Figure 3. The lines represent theoretical scattering functions. Chain line: random walk linear polymer; full line: random walk 18-arm star (eq 3); dashed line: uniform segment density sphere. $\langle S^2\rangle = 4.8 \times 10^5$ Å^2 for all cases.

Table III

A. Hydrodynamic Data for Star Polystyrenes

sample	$s_0^\circ \times 10^{13}$, cm²/s	$[f] \times 10^5$, cm	h[a]	h_{rw}[b]	$r_f \times 10^6$,[c] cm	$r_f/\langle S^2\rangle^{1/2}$
		Cyclohexane, 35 °C				
12-PS1B1A	43.1	8.05	0.81	0.62	4.26	1.23
18-PS1	58.5	9.57	0.76	0.53	5.08	1.27
		Toluene, 35 °C				
12-PS1B1A	36.1	11.7	0.70		6.20	1.08
18-PS1	45.5	14.9	0.68		7.90	1.14

B. Hydrodynamic Data for Star Polystyrenes

sample	$[\eta]$, mL/g	g'[d]	m[e]	$r_\eta \times 10^6$,[f] cm	r_η/r_f
		Cyclohexane, 35 °C			
12-PS1B1A	79.5	0.41	0.62	4.11	0.96
18-PS1	86.5	0.35	0.58	4.96	0.98
		Toluene, 35 °C			
12-PS1B1A	271	0.35	0.82	6.29	1.02
18-PS1	320	0.26	0.74	7.78	0.98

[a] Equation 12. [b] Equation 13. [c] Equation 14. [d] Equation 16. [e] Equation 17. [f] Equation 18.

random walk model scattering curves of linear polymers and 18-arm regular stars are included as is that for a sphere with uniform segment density having the same radius of gyration as 18-PS1. From Figure 4 it can be seen that the experimental $1/P(\mu)$ curve of the star lies between the random walk curve for a regular 18-arm star and that for the uniform-density sphere. Similar data were obtained with 12-PS1B1A in toluene. The phenomenon seems quite general as it was also observed, albeit less clearly, for 12-arm polyisoprenes in the good solvent cyclohexane.[14]

The second virial coefficients A_2 ((cm³·mol)/g²) of the stars in toluene are given in Table II. The values are much smaller than those of linear polymers of similar molecular weight or radius of gyration.

Table III collects the intrinsic viscosities $[\eta]$ and sedimentation velocity coefficients, s_0°, for the stars measured in cyclohexane and in toluene. The intrinsic friction coefficients of the polymers, $[f]$, are calculated from the sedimentation velocity coefficients by

$$[f] = \frac{f}{\eta_0} = \frac{M_w(1 - \bar{v}_2\rho_0)}{s_0^\circ N_A \eta_0} \quad (5)$$

where η_0 and ρ_0 are the solvent viscosity and density, respectively, and $\bar{v}_2$ is the partial specific volume of the polymer in the solvent.

Discussion

A. Polymer Analysis. As was shown, it is possible to analyze highly branched regular star polymers qualitatively for their homogeneity in branch structure and molecular weight with complementary ultracentrifugation sedimentation and GPC–LALLS. The former method resolves a sample into individual components and allows an estimate of the weight fraction of each component; the latter method supplies molecular weights. Such analysis is aided significantly by the near-monodispersity of the precursor and the individual species of star molecules. It should be remarked that these very high molecular weight stars passed through the GPC–LALLS system apparently undegraded, in contrast with the behavior of linear polymers of similar molecular weight.[14]

Although strictly speaking number-average molecular weights have to be used, we have to rely on weight averages for the determination of the number of branches of the stars according to $p = (M_w)_{star}/(M_w)_{arm}$. However, the error so introduced should be within the experimental error for narrow molecular weight distribution polymers. The number of arms given in Table I agrees within experimental error with the functionality of the linking agents.

The molecular weight ratio of 12-PS1C and the 12-arm-star precursor (Figure 1) suggests that 12-PS1C is mainly 9-arm-star material. An analysis of the early stages of the sedimentation of 12-PS1 in cyclohexane indicates that the higher molecular weight fraction sediments 1.14 times faster than the lower molecular weight impurity. Without taking into account concentration and branched structure effects, one calculates that in cyclohexane, where $s_0^\circ = KM^{1/2}$, the 12-arm star will sediment 1.15_5 times faster than the 9-arm star. The fact that no 10- and 11-arm stars are apparent in 12-PS1 suggests that the linking reaction of the living polymer ends with the multifunctional silicon chloride goes to completion. The 9-arm-star polymer could then originate from the presence of an impurity in the dodecachlorosilane, presumably a molecule with one $SiCl_3$ group missing.

B. Star Polymer Conformation. Because the light scattering experiments had to be performed at very low concentrations, it could not be accurately ascertained that $A_2 = 0$ in cyclohexane at 34.6 °C for the star polymer. Our further discussion, however, is based on this assumption. From the experimental $\langle S^2\rangle_\theta$ values, which are, strictly speaking, z averages, g_θ was calculated according to

$$g_\theta = [\langle S^2\rangle_\theta/\langle S^2\rangle_{0,lin}]_M \quad (6)$$

where $\langle S^2\rangle_{0,lin} = 7.9 \times 10^{-18} M_w$ for polystyrene.[3] The g_θ values for the 12- and 18-arm stars are compared with the random walk values (eq 4) in Table II. It can be seen that $g_\theta > g_{rw}$, indicating that these star polymers are expanded at the Θ temperature. This is different from observations on 4- and 6-arm stars.[3,15,16] The Θ temperature expansions, $\alpha_\theta^2 = g_\theta/g_{rw}$, are given in Table II. The value for 12-PS1B1A is lower than the 1.4 value found for 12-arm-star polyisoprenes.[13] It is difficult to say at this point whether this is a genuine difference due to differences in the polymer–solvent pair or whether this must be ascribed to experimental errors. Similar Θ-temperature expansions of divinylbenzene–polystyrene stars were observed.[17] The agreement with the present results must be somewhat fortuitous as those data are based on a quite different $\langle S^2\rangle_{0,lin}$–$M$ relation, $\Theta_{A_2} < \Theta$, and the divinylbenzene-linked stars have larger molecular weight distributions as seen in their ultracentrifugation sedimentation patterns.[14]

Candau et al.[18] have suggested that the expansion of branched polymers at the Θ temperature is due to residual triple contacts and given by

$$\alpha_\Theta^8 - \alpha_\Theta^6 = {}^2/_3 C_{M,l}'({}^1/_3 - \chi_2) g_{tw}^{-3} \quad (7)$$

where $C_{M,l}'$ contains polymer and solvent constants only. From the present data the value of the interaction parameter ${}^1/_3 - \chi_2 = 5 \times 10^{-3}$ is derived. This is quite different from the value 4.5×10^{-2} derived from the Θ_{A_2} temperature depression of 4- and 6-arm stars.[15] In the case of polyisoprene stars ${}^1/_3 - \chi_2$ values from Θ_{A_2} and α_g^2 are in rather good agreement.[13]

Recently, a Monte Carlo computation of the configuration of regular combs was made and the g_{MC} values for stars with many arms were also derived.[19] It can be seen from Table II that g_Θ are somewhat smaller than g_{MC} in the case of polystyrenes while the previously obtained g_Θ data for polyisoprene stars with 8- and 12-arms agree fairly well with the g_{MC} values.[13,19]

In a recent theoretical study of the conformation of stars, the effect of increased segment density near the central branch point was taken into account.[20] The central part of the star consists of a hard core where the monomer concentration is of order unity. Further out from the center the monomer concentration is typical of a semidilute solution. In the outer region of the star with sufficiently long branches, the conformation is that of isolated chains. From this model it was derived that $g_\Theta p^{1/2}$ will be independent of p.[20] The $g_\Theta p^{1/2}$ values are given in the last column of Table II. For 4- and 6-arm polystyrene stars, $g_\Theta p^{1/2} = 1.26$ and 1.13, respectively.[3,15] It appears, therefore, that there is a small residual decrease of $g_\Theta p^{1/2}$ with increasing p. This decrease is less in the case of polyisoprene stars.[20]

Although the radii of gyration of the 12- and 18-arm stars are larger at the Θ temperature than the random walk model predicts, their scattering curve follows closely the theoretical curve base on that model (Figure 3). This indicates that the expansion at the Θ temperature does not cause a profound perturbation from the Gaussian segment distribution, at least not at the large distances viewed by the light scattering experiments. It is, of course, possible that compensating effects cancel each other (vide infra).

In the good solvent toluene, a strong *upward* departure of the $1/P(\mu)$ function from the Gaussian model is observed when $\mu > 4$. No such deviation was found in the scattering curves of 4- and 6-arm stars.[8]

Downward departures from the scattering curve based on the random walk model have been observed for linear polymers in good solvents when $\mu > 5$–10,[21-25] and an example is shown in Figure 5. In the case of linear polymers, the observed downward departure is the result of two opposing effects.[21] The ϵ effect is caused by the fact that in good solvents, the average segment–segment distance, $\langle r_{ij} \rangle$, depends no longer linearly on the number of segments separating i and j but rather

$$\langle \bar{r}_{ij}^2 \rangle \propto |i - j|^{1+\epsilon} \quad (8)$$

where $0 < \epsilon < 0.2$. This effect alone will produce a downward curvature from that for the random walk model ($\epsilon = 0$). The segment density distribution, $\phi(r/\langle r_{ij} \rangle)$, around the average distance $\langle r_{ij} \rangle$ is no longer Gaussian ($t = 2$) but narrower; i.e., it is better represented by $t > 2$ in

$$\phi(r/\langle r_{ij} \rangle) \propto \exp[-(r^2/\langle \bar{r}_{ij}^2 \rangle)^{t/2}] \quad (9)$$

making the segment density distribution more uniform and producing an upward curvature from that for the random walk model. In linear polymers the ϵ effect is obviously stronger than the t effect.

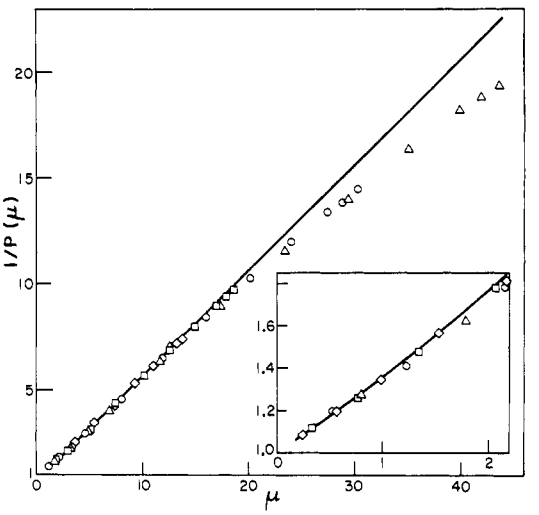

Figure 5. Inverse scattering function against μ for a narrow molecular weight distribution linear polymer. $M = 6.8 \times 10^6$. Solvent: toluene. $\langle S^2 \rangle = 1.7 \times 10^6$ Å^2. (△, □, and ○) As in Figure 3; (◇) 633-nm light. The line is for a random walk chain. The insert shows the data at low μ values.

If the same two phenomena operate in the case of star polymers, then the t effect must be dominant. From the available part of the $1/P(\mu)$ function, no separation between the ϵ and t effects can be made. Since $g_{Tol} < g_\Theta$ (Table II), stars with many arms expand less than the linear polymer with the same number of segments.[19] It is thus conceivable that the value of ϵ is less for those stars. On the other hand, the crowding of segments inside the coils of highly branched stars may produce a spatially limited segment density distribution around $\langle r_{ij} \rangle$, thereby reinforcing the t effect.

By Fourier transformation it is possible to obtain the average segment–segment distribution in the polymer coil, $W(r)$, from the scattering function.[24,26] If one considers only deviations of the actual segment density distribution from the Gaussian one

$$\Delta W(r) = \frac{1}{2\pi^2 r} \int_0^\infty h \Delta P(h^2) \sin(hr)\, dh \quad (10)$$

where $\Delta P(h^2) = P(h^2) - P_{Gaussian}(h^2)$ and $h = (4\pi/\lambda') \sin(\theta/2)$. Qualitatively, it can be said that the observed departure of the scattering curve from that of the random walk model reflects a decreased segment density distribution for intersegmental distances $\langle r_{ij} \rangle$ smaller than about 500 Å and a slight increase of segment–segment distances when $700 < \langle r_{ij} \rangle < 1000$ Å, i.e., of the order of the radii of gyration. The range of distances over which differences in the segment density distribution occur depends to some extent on the unknown continuation of the experimental $P(\mu)$ function at $\mu > 5 \times 10^{-5}$ cm^{-1}, which is not accessible with light scattering. It would be interesting to use neutron scattering to expand the range of scattering vectors and probe the shorter segment–segment distances in these star molecules.

It should be pointed out that the observed departures of the $P(\mu)$ function from that for the random walk one represent minimum values, since residual molecular weight polydispersity and structural variations will lower the experimental $1/P(\mu)$ function.

In Table II, the second virial coefficients, A_2, for the star polymers in toluene are given. These values are 2 and 2.5 times lower than those for linear polymers of the same molecular weight in the case of the 12-arm and 18-arm star,

respectively. The values of the noninterpenetration function ψ[27]

$$\psi = \frac{A_2M^2}{4\pi^{3/2}\langle S^2\rangle^{3/2}} \tag{11}$$

given in Table II are much higher than the limiting value for linear polymers in good solvents (~0.26) and approach the value for a hard sphere (1.61).[27]

The scaling concept leads to the conclusion that $gp^{4/5}$ is a constant for regular stars in a good solvent.[20] Values of $gp^{4/5}$ are given in Table II. The corresponding values for 4- and 6-arm-star polystyrenes are 1.94 and 1.93, indicating that within experimental error $gp^{4/5}$ is indeed constant.

C. Hydrodynamic Properties of Stars. Sedimentation velocity coefficients and intrinsic viscosities of star polystyrenes with 4 and 6 arms have been studied previously for the cases of the Θ solvent (cyclohexane, 35 °C) and the good solvent (toluene, 35 °C). The data on the 12- and 18-arm stars, which are collected in Table III, can now be used to extend a number of relations previously observed between the various properties to regular stars with a higher number of arms.

The sedimentation velocity coefficients of the stars are compared with those of linear polymers of the same molecular weight by

$$h = \frac{(s_0^\circ)_{lin}}{(s_0^\circ)_{star}} = \frac{[f]_{star}}{[f]_{lin}} \tag{12}$$

Assuming the random walk model for chains and Kirkwood–Riseman hydrodynamic interactions between chain segments, one can calculate for regular stars[28]

$$h_{rw} = p^{1/2}[2 - p + 2^{1/2}(p - 1)]^{-1} \tag{13}$$

The comparison in Table IIIa shows that the experimental values of h (eq 12) are larger than the calculated ones, especially in the Θ solvent. In fact, $h \approx h_{rw}^{1/2}$. This was also found with 4- and 6-arm stars.[10]

The radii of the equivalent spheres, i.e., spheres with the same intrinsic friction coefficients as the polymer molecules, can be obtained by Stokes' law

$$r_f = [f]/6\pi \tag{14}$$

These hydrodynamic radii are given in the sixth column of Table IIIa and compared with the radii of gyration of the polymers in the next column.

Traditionally, the relation between the intrinsic friction coefficient of a polymer and its radius of gyration has been expressed by[29]

$$[f] = P'\langle S^2\rangle^{1/2} \tag{15}$$

The P' values (Table IV) of the stars increase with the number of arms from the value for linear polymers to the value for a hard sphere.

It has been pointed out that deviations from the random walk model would be equally found in the conformational property $\langle S^2\rangle$ and the hydrodynamic property and that $h/g^{1/2}$ derived from experiments would be approximately equal to $(h/g^{1/2})_{rw}$.[30] However, for the 12- and 18-arm stars $h/g_\Theta^{1/2} = 1.54$ and 1.59, respectively, compared with 1.28 and 1.33 for $(h/g^{1/2})_{rw}$. Similar discrepancies are found in toluene. The larger experimental ratios were already observed for 4- and 6-arm polystyrene stars.[10]

From the intrinsic viscosity data in Table IIIb one can derive

$$g' = [\eta]_{star}/[\eta]_{lin} \tag{16}$$

Table IV
Hydrodynamic Constants for Regular Stars (Θ Solvent)

type	P' [a]	ϕ' $\times 10^{-25}$ [b]	$\phi'^{1/3}/P'$ $\times 10^{-6}$ [c]
linear	15.0	0.39	2.26
linear theoretical	12.5[d]	0.39[e]	2.7
4-arm star	17.5	0.55	2.17
6-arm star	20.4	0.77	2.08
12-arm star	23.3	1.05	2.03
18-arm star	23.9	1.20	2.06
hard-sphere limit[f]	24.3	1.35,	2.11

[a] Equation 15. [b] Equation 19 with $[\eta]$ in mL/g. [c] ϕ' with $[\eta]$ in dL/g. [d] Reference 27, p 272. [e] Reference 27, p 298 (Pyun-Fixman value). [f] Reference 27, p 351.

at constant molecular weight. Values of g' in the Θ solvent are given in Table IIIb. They are always lower than those proposed theoretically according $g' = g_{rw}^{1/2}$[31] but higher than those proposed according $g' = h_{rw}^3$.[28] These discrepancies were already observed for stars with 4 and 6 arms.[3,15] However, for all regular star polymers it is found that $m \approx 0.58$ in the relation

$$g_\Theta' = g_{rw}^m \tag{17}$$

and this exponent seems to be a lower limit for branched polymers. Indeed, m values for combs are larger than 0.58 and tend to this value when the branches are very large (starlike combs).[32] Values of m in a good solvent are always higher than the Θ solvent value.

The radius of the spherical partical that produces the same increase in viscosity as the polymer is given by

$$r_\eta = (3M[\eta]/10\pi N_A)^{1/3} \tag{18}$$

The equivalent hydrodynamic radii from viscosity (r_η) for the 12- and 18-arm stars are given in Table IIIb. It can be seen that r_η and r_f data are identical within experimental error as was found previously for linear, 4-arm and 6-arm stars, and combs.[10]

The direct relation between $[\eta]$ and $\langle S^2\rangle$ is of the form[29]

$$[\eta]M = \phi'\langle S^2\rangle^{3/2} \tag{19}$$

Values of ϕ' for star polystyrenes are collected in Table IV. The increases of ϕ' values with increasing number of arms in the stars leads to ϕ' values near that for the hard sphere. The ratio $\phi'^{1/3}/P'$ is remarkably constant and allows calculation of s_0° from $[\eta]$ and vice versa.

Acknowledgment. We acknowledge the skillful help of Mr. P. M. Toporowski. Drs. M. Daoud and J. P. Cotton provided a copy of their paper (ref 20) prior to publication. The work done at the Institute of Polymer Science was supported by the Polymers Program, National Science Foundation (Grant No. DMR79-008299).

Registry No. Polystyrene, 9003-53-6.

References and Notes

(1) Bauer, B.; Fetters, L. J. *Rubber Rev.* **1978**, *51*, 406.
(2) Bywater, S. *Adv. Polym. Sci.* **1979**, *30*, 90.
(3) Roovers, J.; Bywater, S. *Macromolecules* **1974**, *7*, 443.
(4) Quack, G.; Fetters, L. J.; Hadjichristidis, N.; Young, R. N. *Ind. Eng. Chem. Res. Dev.* **1980**, *19*, 587.
(5) Hadjichristidis, N.; Guyot, A.; Fetters, L. J. *Macromolecules* **1978**, *11*, 668.
(6) Hadjichristidis, N.; Fetters, L. J. *Macromolecules* **1980**, *13*, 191.
(7) Schachman, H. K. "Ultracentrifugation in Biochemistry"; Academic Press: New York, 1959.

(8) Toporowski, P. M.; Roovers, J. *Macromolecules* **1978**, *11*, 365.
(9) Utiyama, H. In "Light Scattering from Polymer Solutions"; Hughes, M. B., Ed.; Academic Press: London, 1972.
(10) Roovers, J.; Toporowski, P. M. *J. Polym. Sci., Polym. Phys. Ed.* **1980**, *18*, 1907.
(11) Benoit, H. *J. Polym. Sci.* **1953**, *11*, 507. Kolbovskii, Yu. Ya. *Polymer Sci. USSR (Engl. Transl.)* **1962**, *3*, 326.
(12) Zimm, B. H.; Stockmayer, W. H. *J. Chem. Phys.* **1949**, *17*, 1301.
(13) Bauer, B. J.; Hadjichristidis, N.; Fetters, L. J.; Roovers, J. *J. Am. Chem. Soc.* **1980**, *102*, 2410.
(14) Roovers, J., unpublished results.
(15) Roovers, J.; Bywater, S. *Macromolecules* **1972**, *5*, 384.
(16) Hadjichristidis, N.; Roovers, J. *J. Polym. Sci., Polym. Phys. Ed.* **1974**, *12*, 2521.
(17) Zilliox, J.-G. *Makromol. Chem.* **1972**, *156*, 121.
(18) Candau, F.; Rempp, P.; Benoit, H. *Macromolecules* **1972**, *5*, 627.
(19) McCrackin, F. L.; Mazur, J. *Macromolecules* **1981**, *14*, 1214.
(20) Daoud, M.; Cotton, J. P. *J. Phys.* **1982**, *43*, 531.
(21) McIntyre, D.; Mazur, J.; Wims, A. M. *J. Chem. Phys.* **1968**, *49*, 2887, 2896.
(22) Utiyama, H.; Tsunashima, Y.; Kurata, M. *J. Chem. Phys.* **1971**, *55*, 3133.
(23) Smith, T. E.; Carpenter, D. K. *Macromolecules* **1968**, *1*, 204.
(24) Mijnlieff, P. F.; Coumou, D. J.; Meisner, J. *J. Chem. Phys.* **1970**, *53*, 1775.
(25) Utiyama, H.; Utsumi, S.; Tsunashima, Y.; Kurata, M. *Macromolecules* **1978**, *11*, 506.
(26) Carpenter, D. K. *J. Chem. Phys.* **1972**, *56*, 1014.
(27) Yamakawa, H. "Modern Theory of Polymer Solutions"; Harper and Row: New York, 1971.
(28) Stockmayer, W. H.; Fixman, M. *Ann. N.Y. Acad. Sci.* **1953**, *57*, 334.
(29) Mandelkern, L.; Flory, P. J. *J. Chem. Phys.* **1958**, *29*, 311.
(30) Berry, G. C. *J. Polym. Sci., Part A-2* **1968**, *6*, 1551.
(31) Zimm, B. H.; Kilb, R. W. *J. Polym. Sci.* **1959**, *37*, 19.
(32) Roovers, J. *Polymer* **1979**, *22*, 843.

Scaling Relations for Aqueous Polyelectrolyte–Salt Solutions. 1. Quasi-Elastic Light Scattering as a Function of Polyelectrolyte Concentration and Molar Mass

Rudolf S. Koene and Michel Mandel*

Department of Physical and Macromolecular Chemistry, Gorlaeus Laboratories, University of Leiden, 2300 RA Leiden, The Netherlands. *Received April 23, 1982*

ABSTRACT: Quasi-elastic light scattering experiments are reported on sodium poly(styrenesulfonate) solutions in aqueous 0.01 M NaCl. Samples of three different molar masses have been investigated as a function of the macromolecular concentration covering the dilute and the semidilute regimes. Experimental homodyne intensity autocorrelation functions of the scattered light were found to be nonexponential and had to be fitted with the help of a cumulant expansion using a floating value for the base line. From the value of the first cumulant an effective translational diffusion coefficient was evaluated. This diffusion coefficient exhibits a different behavior according to the concentration regime considered. In the dilute regime it is molar mass dependent but only slightly increases with concentration. In the semidilute regime the predictions of the scaling approach to the cooperative diffusion seem to be confirmed. The effective diffusion coefficient is molar mass independent and increases with concentration according to a power law that is close to the theoretically predicted one if adequate corrections for the change of the ionic strength of the solution with the polyelectrolyte concentration are applied. The experimentally found concentration power, larger than the theoretical value of 0.75, depends, however, on the value of the intrinsic persistence length of the polyelectrolyte (theoretically treated as a wormlike chain), which enters the correction factor mentioned. The results therefore seem to confirm that in the semidilute regime investigated a cooperative diffusion depending on the correlation length of the polyelectrolytes determines the diffusional effects as observed in quasi-elastic light scattering whereas in the dilute regime they depend on the translational behavior of individual chains. Both regimes are separated by a transition region where the effective diffusion coefficient seems to be molar mass and concentration dependent.

Introduction

Quasi-elastic light scattering provides a useful technique for determining the diffusion of macromolecules in solution. In the case of neutral polymers in good solvents it has been predicted that according to the concentration regime considered, different diffusion coefficients should be measured:[1] below a critical concentration c^*, which represents the concentration at which the individual chains in solution start to overlap considerably, the diffusion coefficient of the individual chains is measured. It is controlled by the averaged dimension of the macromolecular coils, for which the Flory limit of the radius of gyration may be taken as the characteristic quantity.[2] Above c^* intermolecular entanglements produce cooperative modes analogous to those of a permanent network. In the resulting cooperative diffusion the characteristic dimension is the correlation length ξ, which represents the average distance between successive entanglements along a chain and which should be independent of the molar mass of the chain but dependent on the concentration according to a $C^{-0.75}$ power law.[3] Several light scattering experiments have been reported in the literature[4-6] for solutions in the semidilute regime. In general, slightly different power dependences with concentration have been found as compared to the theoretical predictions.[7] In some studies also nonexponential behavior of the light scattering correlation function was reported, in contrast to the others.

More recently, Odijk[8] has extended the scaling relation for neutral polymers to the case of semidilute polyelectrolyte solutions with or without added salt. In this approach changes in the flexibility of the macromolecular chain due to charge interactions are taken into account within the context of a wormlike chain model.[9] In the presence of an excess of the added salt the theory predicts behavior of the polyelectrolytes analogous to that of neutral polymers if the necessary corrections for charge interactions are applied. In an earlier short communication we found some confirmation of the theoretical prediction

0024-9297/83/2216-0220$01.50/0